

## SEARCHING FOR SINERGIES BETWEEN MICROREACTORS AND ULTRASOUND

PACS: 43.35.Zc

Navarro-Brull, Francisco J.<sup>1</sup>; Poveda, Pedro<sup>2</sup>; Ruiz-Femenía, Rubén<sup>3</sup>; Bonete, Pedro<sup>1</sup>; Gómez, Roberto<sup>1</sup>; Ramis, Jaime<sup>2</sup>

1 Institut Universitari d'Electroquímica i Departament de Química Física,

2 Departament de Física, Enginyeria de Sistemes i Teoria del Senyal,

3 Departament d'Enginyeria Química, Universitat d'Alacant, Apartat 99, E-03080 Alicante, Spain

Tel.: +34 965 903 748 (R. Gómez);

E-mail (F.J. Navarro-Brull): fj.navarro@ua.es

### ABSTRACT

Micro-sono-reactors are the direct combination of microfluidic devices and ultrasound to achieve more efficient operation and fluid mechanical enhancements. A novel microreactor configuration with an integrated piezoelectric actuator has been studied to optimize the effects of the ultrasound irradiation (sonication). A proper sizing of the microreactor was carried out analytically and subsequently demonstrated through a finite element software package (COMSOL Multiphysics). These results are compared with an experimental study (Kuhn et al., 2011) in which it was observed that working at an optimum frequency helps prevent the system from clogging by avoiding the formation of precipitates within the microchannels.

### RESUMEN

Los micro-sono-reactores son dispositivos de microflujo en que mediante ultrasonidos se persigue un funcionamiento más eficiente y una mejora de las propiedades fluidodinámicas. Se ha analizado una configuración de microrreactor con un actuador piezoeléctrico integrado para optimizar los efectos de la sonicación. Se ha realizado un dimensionamiento analítico del microrreactor que se valida seguidamente con un paquete de software de elementos finitos (COMSOL Multiphysics). Estos resultados se comparan con un estudio experimental (Kuhn et al., 2011) en que se observó que trabajando a una frecuencia óptima se previene la formación de precipitados y la obstrucción de los microcanales del reactor.

## INTRODUCTION AND SCOPE

Microfluidic devices, also known as Lab on a Chip, have gained popularity during the past years. There is an emerging demand of this technology especially in the fine chemistry sector and, more concretely, in the pharmaceutical and food industry. By reducing the diameter of the reactor channels to tens/hundreds of micrometres, the flow conditions change radically. On this scale, laminar flow (i.e. low Reynolds number) is obtained and phenomena such as diffusion, among others, become decisive. In addition to this, the high increase of surface-to-volume ratio allows them to carry out fast exothermic reactions under controlled conditions. As a result, the use of these microreactors leads to *green* production methods if one considers the higher selectivity and reduced waste of compounds that are finally obtained.

Within this framework, the MAPSYN European project aims to bring selected innovative energy-efficient chemical reaction processes by using microreactors and a combination of microwave, ultrasound and plasma. (Hessel et al., 2013)

Despite the extensive potential that ultrasound irradiation (i.e. sonication) is able to achieve by cavitation collapse and associated phenomena such as sonoluminescence, these physicochemical effects will not be overviewed in this study. Instead, the only object of the present analysis will be the use of ultrasounds in an area where they have been largely employed as fluidomechanical agents. One of the main drawbacks that the microfluidics needs to cope with is the formation of precipitates within the microchannels. The use of ultrasonic irradiation to prevent clogging has been successfully implemented with different kinds of configurations ranging from the immersion in ultrasonic baths to the integration of miniaturised piezoelectric transducers. (Fernandez Rivas et al., 2012).

In this context, the acoustic energy is being applied in different forms and with different sizes and geometries. The importance of these configurations and their influence could be overlooked, being the usual workflow to optimise the effects by changing the applied frequency once the device is mounted. The complexity that ultrasonic irradiation and its optimisation involve is not regarded as determinant since their effects are a tool, not an end.

A typical example of this methodology is provided by (Kuhn et al., 2011) where they presented a Teflon stack microreactor with an integrated piezoelectric actuator to prevent it from clogging. In their study, an optimum value of 50 kHz is found after performing a scan over a limited frequency range with a couple of microreactors.

This work aims to provide a simplified strategy to optimize the microreactor from the ultrasonic viewpoint during its design. The results of this approach will be compared with the real case mentioned above.

## REVIEW OF THE EXPERIMENTAL RESULTS

A Teflon stack microreactor (Figure 1) with an integrated piezoelectric actuator has been proposed to study the benefits of ultrasound irradiation by the Department of Chemical Engineering of the MIT (USA). The device was fabricated by assembling PTFE plates of 70x70mm, one of them with an engraved microchannel of 600  $\mu\text{m}$ , and compressing them between two stainless steel chucks. A piezoelectric sheet of 1 mm thickness (Piezo Systems, Inc.) was encased in one of the PTFE plates and was driven at different frequencies by a wave generator (Agilent 33120A) and an amplifier (ENI 1040L power amplifier) at a load power of 30 W.

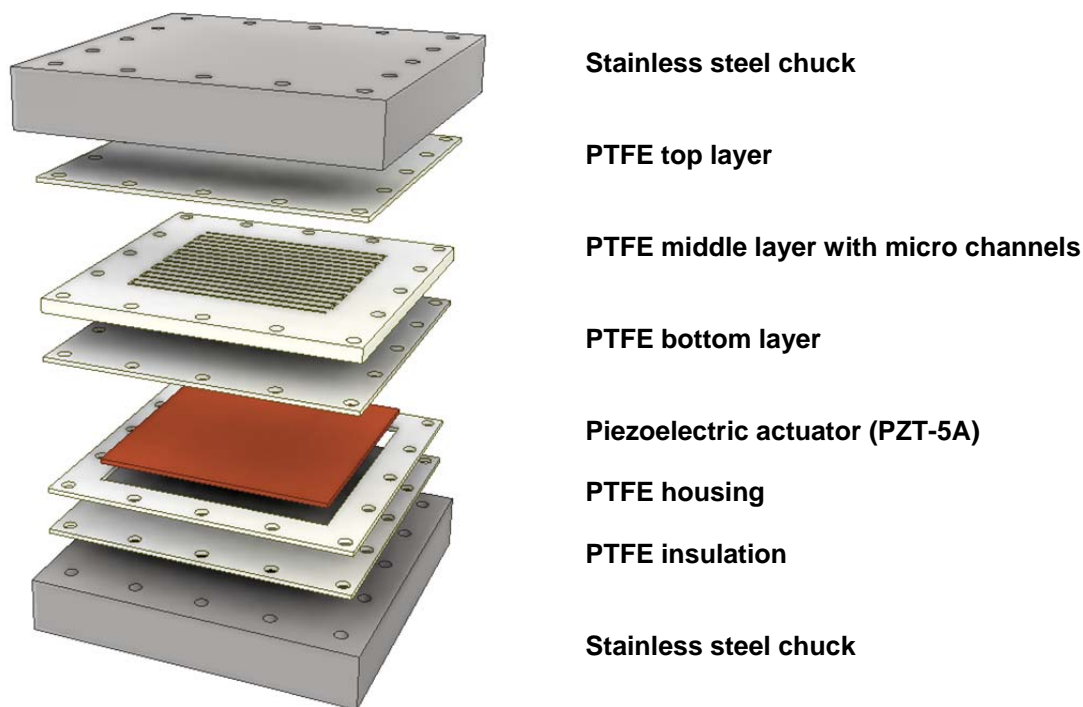


Figure 1. Representation of the assembly constituting the Teflon-stacked microreactor. See text for details.

The resulting micro-sono-reactor was tested under microflow conditions to carry out Pd-catalysed couplings of anilines and aryl halides. These coupling reactions are extensively used in industry and academia due to their versatility. In fact, they could be considered as one of the most important synthetic methodologies developed in the past 15 years. However, inorganic by-products, such as NaCl and NaBr, precipitate instantly due to their insolubility in the non-polar solvent where these reactions take place. Hence, the microchannels where the reaction occurs are prone to be clogged by these solids, which make ultrasound irradiation a necessity. By analyzing the particle size distribution, an optimum ultrasound frequency of 50 kHz was found. In fact, the maxima of the particle size distribution were located respectively at 30, 9, and 13  $\mu\text{m}$  upon sonication at 40, 50 and 60 kHz.

## SIZING OPTIMIZATION

By means of an equivalent circuit, a Langevin-type transducer can be optimized to get the maximum of the acoustic pressure in the liquid reactant filling the microchannel. In order to obtain a simplified model, a series of assumptions have been made.

First, we suppose that there are solely plane-wave propagations through the longitudinal section of the reactor, where the tension in the interior of the pieces is evenly distributed throughout their cross section. Thus, the model will be reduced to a 2D section of the stacked microreactor.

Second, by considering that the forces exerted by the surfaces on the air by the back and front ends are negligible, the equivalent circuit is simplified to a single impedance. When the system vibrates at the resonance frequency, the impedance of such an equivalent circuit becomes zero, being obtained Equation 1 for the resonant frequency of a Langevin-type ultrasonic transducer (Radmanović & Mančić, 2004).

$$k_p l_p + \tan^{-1} \left( \frac{Z_b^c}{Z_p^c} \tan k_b l_b \right) + \tan^{-1} \left( \frac{Z_f^c}{Z_p^c} \tan k_f l_f \right) = \pi \quad \text{Equation 1}$$

where  $k$  denotes the angular wavenumber ( $2\pi/\lambda$ ) and  $Z$  the acoustic impedance ( $\rho c$ ) of each section. The first term of Equation 1 corresponds to the piezoelectric crystal, and the second and third terms to the back and front side, respectively. Consequently,  $l_p$  is the thickness of the piezoelectric material, while  $l_b$  and  $l_f$  are the thicknesses of the Teflon layer below and above it, respectively.

It is necessary to define the alignment of the piezoelectric ceramic, the back, and front of the transducer, because the former should be located at a node, allowing the longitudinal displacement of the transducer to be transmitted without affecting the resonant frequency of the system.

Hence, the transducer can be divided into two sections from the node, with each section representing a quarter of the wavelength of the resonator. In this way, Equation 1 can be split into Equation 2 and Equation 3.

$$k_p l_p + \tan^{-1} \left( \frac{Z_b^c}{Z_p^c} \tan k_b l_b \right) = \frac{\pi}{2} \quad \text{Equation 2}$$

$$\tan^{-1} \left( \frac{Z_f^c}{Z_p^c} \tan k_f l_f \right) = \frac{\pi}{2} \quad \text{Equation 3}$$

Finally, it must be underlined that the two stainless steel chucks closing the microreactor are not considered in this sizing. The transducer is modelled to have a maximum output at the back side where, due to the impedance differences between Teflon and stainless steel, the transmission of the vibration will be insignificant (~97% of reflection). In contrast, on the front side the width of Teflon is designed to have a maximum within the microchannel. However, the interface between Teflon and stainless steel on the front side will be located at a node, where the vibration is zero and therefore not interfering with the signal.

## NUMERICAL MODEL (2D)

The acoustic field within the liquid microchannel and the deformation of the stacked microreactor have been calculated by following the simulation strategies exposed in the literature (Louisnard et al., 2009; Tudela et al., 2011).

### *Linear Acoustics in the Working Liquid.*

The governing equations for a compressible lossless fluid flow medium are the momentum equation and the continuity equation. Assuming mono-harmonic vibrations, the wave equation for acoustic waves can be reduced to Equation 4, known as the Helmholtz equation.

$$\nabla^2 p + \left( \frac{\omega}{c} \right)^2 p = 0 \quad \text{Equation 4}$$

where  $p$  is the acoustic pressure,  $c$  is the speed of sound in the liquid and  $\omega$  is the angular frequency. At the channel wall, the continuity condition has been applied as boundary condition to set the interaction from fluid to solid and vice versa (Equation 5).

$$\frac{1}{\rho_l \omega^2} \nabla p \cdot \mathbf{n} = \mathbf{u} \cdot \mathbf{n} \quad \text{Equation 5}$$

where  $\mathbf{n}$  is the outward-pointing unit normal vector seen from inside of the solid domain,  $\rho_l$  is the density of the liquid and  $\mathbf{u}$  is the structural complex amplitude of the displacement field of the solid. Hence, on the boundaries where the fluid interacts with the solid, there is continuity of the normal component of acceleration: the normal component of the acceleration associated with the acoustic pressure on the boundary is equal to the normal component of the acceleration based on the second derivatives of the structural displacements (mono-harmonic vibrations are assumed for the solid).

*Vibration of the Solid.*

Considering that the linear elastic materials present in the microreactor (PTFE and stainless steel) have the same properties in all directions (isotropic), the vibrations transmitted through these solids are calculated by the Equation 6 assuming elastic deformation for all materials, neglecting volume forces and assuming mono-harmonic vibrations:

$$-\rho_s \omega^2 \mathbf{u} = \nabla \sigma, \quad \sigma = \mathbf{s} \quad \text{Equation 6}$$

where  $\rho_s$  is the density of the solid,  $\mathbf{u}$  is the displacement field and  $\sigma = \mathbf{s}$  is the elastic strain tensor given by Equation 7.

$$\mathbf{s} = \frac{E\nu}{(1+\nu)(1-2\nu)} (\text{Tr}\boldsymbol{\varepsilon})\mathbf{I} + \frac{E}{1+\nu} \boldsymbol{\varepsilon} \quad \text{Equation 7}$$

where  $E$  refers to Young's modulus,  $\nu$  is the Poisson's ratio,  $\mathbf{I}$  the identity Tensor and  $\text{Tr}$  the trace operator. The total strain tensor,  $\boldsymbol{\varepsilon}$ , can be written in terms of the displacement gradient in the Equation 8.

$$\boldsymbol{\varepsilon} = \frac{1}{2} (\nabla \mathbf{u} + \nabla \mathbf{u}^T) \quad \text{Equation 8}$$

As boundary conditions for the solid, the continuity at interior boundaries has been applied, whereas at the boundaries in contact with air a free condition is assumed (components of stress equal to zero).

At liquid/solid interfaces, the stress imposed on the solid is equal to the normal pressure stress exerted by the liquid (Equation 9).

$$\sigma \cdot \mathbf{n} = p_t \mathbf{n} \quad \text{Equation 9}$$

Where  $p_t = p + p_0$  is the total pressure evaluated at the interface. As previously stated,  $\mathbf{n}$  is the normal unit vector pointing outward the liquid. Finally, a fixed constraint ( $\mathbf{u} = 0$ ) is set at the ends of the bolts.

A loss factor damping was added to this model to reproduce the inherent damping of the different materials. In particular, the isotropic loss factor used is the ratio of the loss modulus and the Young's storage modulus (Macioce, 2003). In the frequency domain, the stress relaxation function of viscoelastic material is represented by  $(1 + j\eta_s)\mathbf{C}$ , being  $\mathbf{C}$  is the right Cauchy-Green tensor,  $\eta_s$  is the isotropic loss factor and  $j$  is the imaginary unit.

*Piezoelectric Material.*

The piezoelectric is the actuator of the system, transforming an electric voltage to mechanical energy. Within a piezoelectric, a coupling exists between stress, strain, electric field, and the electric displacement, which can be expressed by the in the stress-charge form by Equation 10 and Equation 11:

$$\boldsymbol{\sigma} = \mathbf{c}_E \boldsymbol{\varepsilon} - \mathbf{e}^T \mathbf{E} \quad \text{Equation 10}$$

$$\mathbf{D} = \mathbf{e} \boldsymbol{\varepsilon} + \boldsymbol{\epsilon}_s \mathbf{E} \quad \text{Equation 11}$$

Where,  $\mathbf{c}_E$  is the elasticity matrix,  $\mathbf{e}$  is the coupling matrix,  $\mathbf{E} = -\nabla V$  is the electric field,  $\mathbf{D}$  is the electric displacement field and  $\boldsymbol{\epsilon}_s$  is the permittivity matrix. To make the variables consistent with previous equations, naming convention is changed (i.e. the strain is named  $\boldsymbol{\varepsilon}$  instead of  $\mathbf{S}$ , and the stress is named  $\boldsymbol{\sigma}$  instead of  $\mathbf{T}$ ). The ground ( $V = 0$ ) is placed on the top of the piezoelectric, whereas at the bottom an electric potential of 40 V is applied.

## RESULTS AND DISCUSSION

The model was numerically solved with COMSOL Multiphysics (v. 4.3a), where the Acoustic-Piezoelectric Interaction module was employed in order to obtain the spatial distribution of the acoustic pressure in the working fluid and the deformation of the microreactor. A frequency scan was carried out between 30 kHz and 100 kHz with steps of 100Hz to test the effectiveness of the optimum sizing described above. The liquid in the microreactor tube was water with properties  $\rho = 1000 \text{ kg/m}^3$  and  $c = 1500 \text{ m s}^{-1}$ . The elastic properties were taken as  $E = 0.49 \text{ GPa}$ ,  $\nu = 0.46$ ,  $\eta = 0.042$  for Teflon, and  $E = 205 \text{ GPa}$ ,  $\nu = 0.27$  and  $\eta = 0.0016$  for stainless steel. The piezoelectric material was PZT-5A.

A 2D structured mesh with about 20.000 2nd-order Lagrange elements was used for spatial discretisation of a longitudinal cross-sectional plane. With the aim of resolving the steep gradients occurring in the system displacements, the mesh was refined close into the PZT and the reactant liquid. Thus, the maximum element size in these domains was set to 0.3 mm, whereas it did not exceed 1 mm of size in the rest of the domains. In any case, the number of degrees of freedom (DOFs) per wavelength was in all cases larger than 5, which ensures a good accuracy.

The **Figure 2** shows a maximum of acoustic pressure close to 50 kHz (actually at 53.5 kHz), which was the frequency chosen to perform this optimisation design.

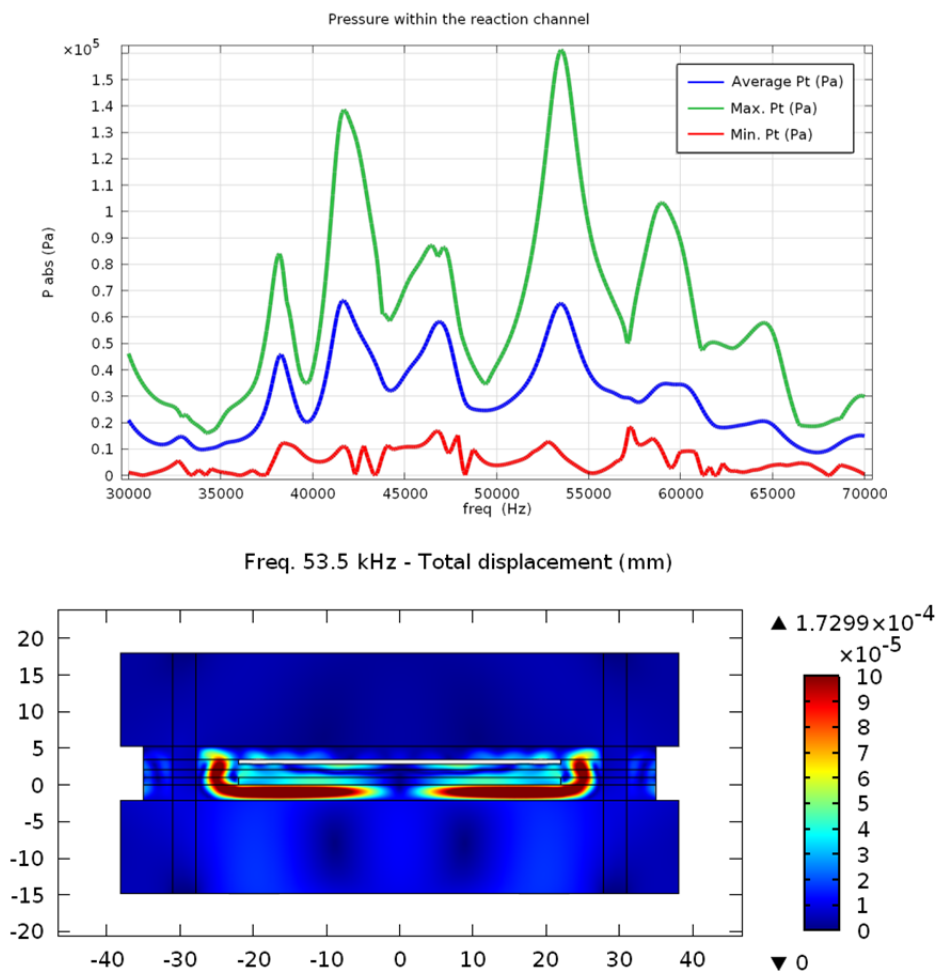


Figure 2. Left: Absolute pressure results in the reactant liquid showing a maximum at 53.5 kHz. Right: Total displacement at 53.5 kHz.

The thicknesses of the Teflon layers in contact with the piezoelectric, calculated with Equation 2 and Equation 3, were respectively  $1.7299 \times 10^{-4}$  mm and  $1.7299 \times 10^{-4}$  mm. However, the original dimensions employed in the experiment were 1 and 3.9 mm, respectively. A 2D sketch with a comparison of both the optimized and actually employed microreactors is shown in Figure 3, highlighting a difference between the above-mentioned original and optimized dimensions. Although not dramatic, such a difference leads to significant advantages allowing the user to choose the desired working frequency according to the particular needs of the system.

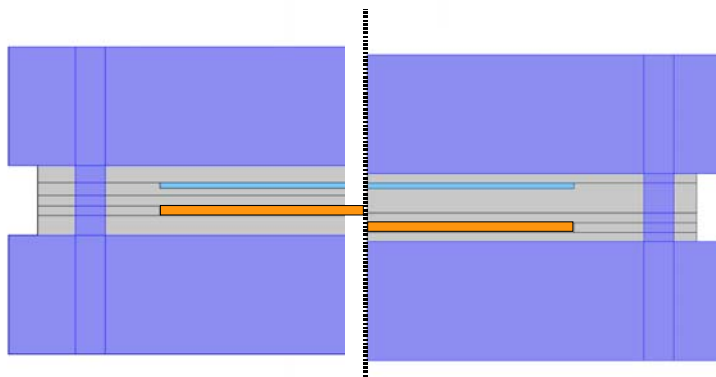


Figure 3. Sketch comparing the dimensions of the optimized (left) and the original microreactor designs (right). Dark blue refers to stainless steel, grey to PTFE, blue to the reactant liquid, and orange to PZT-5A.

## CONCLUSIONS AND OUTLOOK

The present research is motivated by the potential advantages that the incorporation of ultrasound irradiation offers for preventing microreactor-related problems and enhancing their performance. Concretely, an optimisation-oriented microreactor sizing is proposed based on the use of a simple acoustic model, leading to approximate results in the design process. Importantly, our calculations help rationalize experimental results found in the literature (Kuhn et al., 2011). Admittedly, we bear in mind the simplicity of the model presented here. Further work is underway to extend the acoustic simulation from a two-dimensional to a three-dimensional model.

We want to emphasize that a proper acoustic design of the microreactor is preferable over an empirical optimization of the working frequency in a microreactor where the actuator is included *a posteriori*. In fact, the physicochemical effects of ultrasound depend on the frequency being employed. Therefore it is usually important to work at specific frequencies, which demands taking the acoustic design as a crucial part of the microsonoreactor design. In more general vein, this study highlights how the acoustic expertise is receiving an increasing demand in multidisciplinary fields and in particular in Chemistry and Chemical Engineering.

## ACKNOWLEDGEMENTS

This research is funded by the EU project MAPSYN: Microwave, Acoustic and Plasma SYNtheses, under grant agreement No. CP-IP 309376 of the European Union Seventh Framework Program.

## BIBLOGRAPHY

- Fernandez Rivas, D., Cintas, P., & Gardeniers, H. J. G. E. (2012). Merging microfluidics and sonochemistry: towards greener and more efficient micro-sono-reactors. *Chemical communications (Cambridge, England)*, 48(89), 10935–47. doi:10.1039/c2cc33920j
- Hessel, V., Cravotto, G., Fitzpatrick, P., Patil, B. S., Lang, J., & Bonrath, W. (2013). Industrial applications of plasma, microwave and ultrasound techniques: Nitrogen-fixation and hydrogenation reactions. *Chemical Engineering and Processing: Process Intensification*.

- Kuhn, S., Noël, T., Gu, L., Heider, P. L., & Jensen, K. F. (2011). A Teflon microreactor with integrated piezoelectric actuator to handle solid forming reactions. *Lab on a chip*, 11(15), 2488–92.
- Louisnard, O., Gonzalez-Garcia, J., Tudela, I., Klima, J., Saez, V., & Vargas-Hernandez, Y. (2009). FEM simulation of a sono-reactor accounting for vibrations of the boundaries. *Ultrasonics Sonochemistry*, 16, 250–259.
- Maciocce, P. (2003). Viscoelastic damping. *Sound and Vibration*. Retrieved from [http://www.roush.com/portals/1/downloads/articles/sv\\_damping101.pdf](http://www.roush.com/portals/1/downloads/articles/sv_damping101.pdf)
- Radmanović, M., & Mančić, D. (2004). Design and modeling of the power ultrasonic transducers. *Edited by the Faculty of Electronics in Niš, University of Niš, Niš, Serbia*.
- Tudela, I., Sáez, V., Esclapez, M. D., Bonete, P., Harzali, H., Baillon, F. & González-García, J., Louisnard, O. (2011). Study of the influence of transducer-electrode and electrode-wall gaps on the acoustic field inside a sonoelectrochemical reactor by FEM simulations. *Chemical Engineering Journal*, 171(1), 81–91.